Biogeosciences Discuss., https://doi.org/10.5194/bg-2019-97
Manuscript under review for journal Biogeosciences
Discussion started: 26 March 2019

Biogeosciences Discussions Open Access EGU

Ocean acidification and high irradiance stimulate growth of the Antarctic cryptophyte *Geminigera cryophila*

Scarlett Trimborn[1,2], Silke Thoms[1], Pascal Karitter[1], Kai Bischof[2]

[1]EcoTrace, Biogeosciences section, Alfred Wegener Institute, Bremerhaven, 27568, Germany
[2]Marine Botany, Department 2 Biology/Chemistry, University of Bremen, Bremen, 28359, Germany

Correspondence to: Scarlett Trimborn (scarlett.trimborn@awi.de)

Abstract.

Ecophysiological studies on Antarctic cryptophytes to assess whether climatic changes such as ocean acidification and enhanced stratification affect their growth in Antarctic coastal waters in the future are lacking so far. This is the first study that investigated the combined effects of increasing availability of pCO_2 (400 and 1000 µatm) and irradiance (20, 200 and 500 µmol photons m^{-2} s^{-1}) on growth, elemental composition and photophysiology of the Antarctic cryptophyte *Geminigera cryophila*. Under ambient pCO_2, this species was characterized by a pronounced sensitivity to increasing irradiance with complete growth inhibition at the highest light intensity. Interestingly, when grown under high pCO_2 this negative light effect vanished and it reached highest rates of growth and particulate organic carbon production at the highest irradiance compared to the other tested experimental conditions. Our results for *G. cryophila* reveal beneficial effects of ocean acidification in conjunction with enhanced irradiance on growth and photosynthesis. Hence, cryptophytes such as *G. cryophila* may be potential winners of climate change, potentially thriving better in more stratified and acidic coastal waters and contributing in higher abundance to future phytoplankton assemblages of coastal Antarctic waters.

1 Introduction

Even though Antarctic coastal waters comprise a relatively small area relative to the open ocean, these waters are highly productive due to the constant supply of macronutrients and iron (Arrigo et al., 2008). Shelf waters adjacent to the Western Antarctic Peninsula (WAP) are currently undergoing rapid physical changes, exhibiting the most rapid warming rates than anywhere in Antarctica over the last decades (Ducklow et al., 2007, 2013). Rising air temperature resulted in shorter sea ice seasons (Smith and Stammerjohn, 2001) with contrasting effects on phytoplankton biomass, composition and productivity between the northern and southern WAP. In contrast to the southern part, northern WAP waters were found to exhibit both reduced chlorophyll *a* accumulation (Montes-Hugo et al., 2009) and primary production (Moreau et al., 2015), these trends were explained by reduced ice cover, exposing surface waters to greater wind activities and deepening thereby the upper mixed layer. Deeper mixed waters provide less favorable light conditions, potentially explaining the measured decline of large phytoplankton such as diatoms relative to the whole community (Montes-Hugo et al., 2009; Rozema et al., 2017). Accordingly, a recurrent shift from diatoms to cryptophytes and small flagellates was reported for this region, with important implications for food web dynamics (Moline et al., 2004; Ducklow et al., 2007; Montes-Hugo et al., 2009; Mendes et al., 2017). The frequent occurrence of cryptophytes was previously reported after diatom blooms (Moline and Prezelin, 1996) and was related to surface melt water stratification (Moline et al., 2004). As a result from rising global air temperatures, surface water freshening is expected to shallow the upper water layer, exposing

phytoplankton to higher light intensity (Moreau et al., 2015). Relative to diatoms and the prymnesiophyte *Phaeocystis antarctica*, cryptophytes were found to be the main contributors to biomass in stratified and warm WAP coastal waters potentially resulting from their high tolerance to withstand high irradiances (Mendes et al., 2017). Considering the lack in ecophysiological studies carried out with Antarctic ecologically relevant cryptopyte species it remains yet unclear whether the projected climatic changes could promote cryptophyte growth in Antarctic coastal waters in the future.

Phytoplankton productivity can be enhanced through increased light, but can also be impacted by excessive radiation causing photoinhibition and cell damage. Cryptophytes are exceptional among eukaryotic microalgae as they contain similar to diatoms chlorophyll a/c proteins, the carotenoid alloxanthin and phycobiliproteins homologous to red algal phycobiliproteins (Gould et al., 2008). This pigment composition allows crypotophytes to cope well under limited irradiance. Different to diatoms and prymnesiophytes, cryptophytes have no photoprotective de-epoxidation/epoxidation cycling of xanthophyll pigments (e.g. diadinoxanthin, diatoxanthin), instead they rely on chlorophyll a/c proteins, which function to dissipate excess light energy, as another type of nonphotochemical quenching (NPQ; Funk et al., 2011; Kana et al., 2012). While laboratory studies so far mainly have concentrated to disentangle the physiological response of Southern Ocean key species of diatom and prymnesiophytes to different environmental factors Antarctic cryptophytes have received so far little attention. Apart from field studies (Moline et al., 2004; Ducklow et al., 2007; Montes-Hugo et al., 2009), almost nothing is known on how climate change could influence the ecophysiology of Antarctic cryptophytes. Due to the increased solubility of CO_2 in cold water, ocean acidification (OA) is anticipated to strongly affect polar waters (Orr et al., 2005; IPCC Report, 2014). Recent studies suggest that Southern Ocean diatoms are more prone to ocean acidification (OA) than the prymnesiophyte *Phaeocystis antarctica*, in particular when exposed to increased irradiance (Feng et al., 2010; Trimborn et al., 2017a,b; Beszteri et al. 2018; Heiden et al., 2018; Koch et al., 2018, Heiden et al., 2019). The response of cryptophytes to OA is hitherto almost unexplored. The few studies on temperate phytoplankton communities suggest that cryptophytes were not affected by OA (Schulz et al., 2017), even when exposed in combination with increased ultraviolet radiation (Domingues et al., 2014) or warming (Sommer et al., 2015). Similarly, no discernible OA effect on cryptophyte abundance was found in subantarctic (Donahue et al., 2019) and Antarctic (Young et al., 2015) natural phytoplankton communities composed of diatoms, cryptophytes, and *Phaeocystis* spp..

Due to the limited information available on cryptophyte physiology, this study assessed OA effects and their interaction with increasing irradiance on the physiology of the Antarctic cryptophyte *Geminigera cryophila*. To this end, *G. cryophila* was grown under two pCO_2 levels (400 and 1000 µatm) in combination with three irradiance levels (20, 200 and 500 μmol photons m^{-2} s^{-1}) and their interactive effects on growth, elemental composition and photophysiology were assessed.

2 Material and Methods

2.1 Culture conditions

For the preacclimation phase (two weeks) and the main experiment, semi-continuous cultures of the Antarctic cryptophyte *Geminigera cryophila* (CCMP 2564) were grown at 2 °C in sterile-filtered (0.2 μm) Antarctic seawater (salinity 30.03). The seawater was enriched with trace metals and vitamins according to F/2 medium (Guillard and Ryther, 1962). Phosphate and nitrate were added in concentrations of 100 and 6.25 μmol L^{-1}, reflecting the Redfield

N:P ratio of 16:1 (Redfield, 1963). *G. cryophila* cells were grown in triplicates at an incident light intensity of 20, 200 and 500 μmol photons m^{-2} s^{-1} (LL, ML and HL treatment, respectively) under a 16:8 h light:dark light cycle using light-emitting diodes (LED) lamps (SolarStinger LED SunStrip Marine Daylight, Econlux). Light intensities were adjusted using a LI-1400 datalogger (Li-Cor, Lincoln, NE, USA) with a 4π-sensor (Walz, Effeltrich, Germany). Additionally, cultures of the three light treatments and the dilution media were continuously and gently bubbled through a frit with humidified air of CO_2 partial pressures (pCO_2) of 400 (ambient pCO_2 treatment) or 1000 μatm (OA treatment, Table 1). CO_2 gas mixtures were generated with a gas flow controller (CGM 2000, MCZ Umwelttechnik, Bad Nauheim, Germany), using CO_2-free air (< 1 ppmv CO_2; Dominick Hunter, Kaarst, Germany) and pure CO_2 (Air Liquide Deutschland ltd., Düsseldorf, Germany). The CO_2 gas mixtures were regularly monitored with a nondispersive infrared analyzer system (LI6252; Li-Cor Biosciences) calibrated with CO_2-free air and purchased gas mixtures of 150 ± 10 and 1000 ± 20 ppmv CO_2 (Air Liquide Deutschland). Dilutions with the corresponding acclimation media ensured that the pH level remained constant (±0.07 units, Table 1) and that the cells stayed in the mid-exponential growth phase. *G. cryophila* cells were acclimated to the respective light and pCO_2 levels for at least two weeks prior to the start of the main experiment. Despite several attempts, *G. cryophila* did not grow at ambient pCO_2 in conjunction with HL. For the main experiments, cells grew in exponential phase and final sampling took place between 7,280 and 17,161 cells per mL.

2.1 Seawater carbonate chemistry

The pH of the different cultures and the culture medium was measured every other day and at the final sampling day using a pH-ion meter (pH-Meter 827, Metrohm), calibrated (3 point calibration) with National Institute of Standards and Technology-certified buffer systems. The pH remained constant at 8.13 ± 0.07 and 7.82 ± 0.06 for the ambient pCO_2 and OA treatments, respectively (Table 1). Dissolved inorganic carbon (DIC) samples were sterile-filtered (0.2 μm) and stored at 4 °C in 5 mL gas-tight borosilicate bottles without headspace until analysis. DIC was measured colourimetrically in duplicates with a QuAAtro autoanalyzer (Seal Analytical, Stoll et al., 2001). The carbonate system was calculated based on DIC, pH, silicate (97 µmol kg^{-1}), phosphate (6.1 µmol kg^{-1}), temperature (2.0 °C) and salinity (30.03) using the CO2Sys program (results shown in Table 1, (Pierrot et al., 2006) choosing the equilibrium constant of Mehrbach et al. (1973) refitted by Dickson and Millero (1987).

2.2 Growth, elemental stoichiometry and composition

Cell count samples of every *G. cryophila* treatment were taken on a daily basis at the same time of day and were determined immediately after sampling using a Coulter Multisizer III (Beckmann-Coulter, Fullerton, USA). Cell-specific growth rate (μ, unit d^{-1}) was calculated as

$$\mu = (\ln N_{fin} - \ln N_0)/\Delta t, \quad (1)$$

where N_0 and N_{fin} denote the cell concentrations at the beginning and the end of the experiments, respectively, and Δt is the corresponding duration of incubation in days.

Particulate organic carbon (POC) and particulate organic nitrogen (PON) were measured after filtration onto precombusted (12 h, 500 °C) glassfibre filters (GF/F, pore size ~0.6 μm, Whatman). Filters were stored at -20 °C and dried for >12 h at 64 °C prior to sample preparation. Analysis was performed using an Euro Vector CHNS-O elemental analyzer (Euro Elemental Analyzer 3000, HEKAtech GmbH, Wegberg, Germany). Contents of POC and PON were corrected for blank measurements and normalized to filtered volume and cell densities to yield cellular

quotas. Production rates of POC and PON were calculated by multiplication of the cellular quota with the specific growth rate of the respective treatment.

2.3 Chlorophyll *a* fluorescence

The efficiency of photochemistry in photosystem II (PSII) was assessed in all treatments using a Fast Repetition Rate fluorometer (FRRf, FastOcean PTX; Chelsea Technologies Group ltd., West Molesey, United Kingdom) in combination with a FastAct Laboratory system (Chelsea Technologies Group ltd., West Molesey, United Kingdom). Cells of the respective treatment were dark-acclimated for 10 min, before minimum chlorophyll *a* (Chl *a*) fluorescence (F_o) was recorded. Subsequently, a single turnover flashlet (1.2 x 10^{22} photons m^{-2} s^{-1}, wavelength 450 nm) was applied to cumulatively saturate photosystem II (PSII), i.e. a single photochemical turnover (Kolber et al., 1998). The single turnover saturation phase comprised 100 flashlets on a 2 μs pitch and was followed by a relaxation phase comprising 40 flashlets on a 50 μs pitch. This sequence was repeated 24 times within each acquisition. The saturation phase of the single turnover acquisition was fitted according to Kolber et al. (1998). From this measurement, the minimum (F_o) and maximum (F_m) Chl *a* fluorescence was determined. Using these two parameters, the dark-adapted maximum PSII quantum yield (F_v/F_m) was calculated according to the equation $(F_m - F_o)/F_m$. During the fluorescence light curve (FLC), cells were exposed for 5 min to eight actinic light levels ranging from 35 to 1324 μmol photons m^{-2} s^{-1}. From these measurements, the light-adapted minimum (F') and maximum (F_m') fluorescence of the single turnover acquisition was estimated. The effective PSII quantum yield under ambient light (F_q'/F_m') was derived according to the equation $(F_m' - F')/F_m'$ (Genty et al., 1989). From this curve, absolute electron transport rates (ETR, e^- $PSII^{-1}$ s^{-1}) were calculated following Suggett et al. (2004, 2009):

$$ETR = \sigma_{PSII} \times (F_q'/F_m' / F_v/F_m) \times E, \quad (2)$$

where σ_{PSII} is the functional absorption cross section of PSII photochemistry and E denotes the applied instantaneous irradiance (photons m^{-2} s^{-1}). Light-use characteristics were analyzed by fitting irradiance-dependent ETRs according to Ralph and Gademann (2005), including maximum ETR (ETR_{max}), minimum saturating irradiance (I_K) and maximum light utilization efficiency (α). Using the Stern-Volmer equation, nonphotochemical quenching (NPQ) of chlorophyll *a* fluorescence was calculated as $F_m/F_m' - 1$. From the single turnover measurement of dark-adapted cells, σ_{PSII}, the energy transfer between PSII units (i.e. connectivity, *P*), the re-oxidation of the electron acceptor Q_a (τ) and the concentration of functional photosystem II reaction centers ([RII]) were assessed from iterative algorithms for induction (Kolber et al., 1998) and relaxation phase (Oxborough, 2012). [RII] represents an estimator for the content of PSII in the sample and was calculated according to the following equation:

$$[RII] = (F_o / \sigma_{PSII}) \times (K_R / E_{LED}), \quad (3)$$

where K_R is an instrument specific constant and E_{LED} is the photon flux from the FRRf measuring LEDs. After the completion of the FLC curve, an additional dark-adaptation period of 10 min was applied, followed by a single turnover flashlet to check for recovery of PSII. Using the F_v/F_m measured before and after the FLC-curve, the yield recovery was calculated and given as % of the initial F_v/F_m (before the FLC-curve). All measurements (n = 3) were conducted at the growth temperature of 2 °C.

2.4 Pigments

Samples for the determination of pigment concentration were filtered onto GF/F filters and immediately frozen at -80 °C until further analysis. Pigments samples were homogenized and extracted in 90% acetone for 24h at 4 °C in

the dark. After centrifugation (5 min, 4 °C, 13000 rpm) and filtration through a 0.45 µm pore size nylon syringe filter (Nalgene®, Nalge Nunc International, Rochester, NY, USA), concentrations of chlorophyll *a* (Chl *a*) and c_2 (Chl c_2), and alloxanthin (Allo) were determined by reversed phase High Performance Liquid Chromatography (HPLC). The analysis was performed on a LaChromElite® system equipped with a chilled autosampler L-2200 and a DAD detector L-2450 (VWR-Hitachi International GmbH, Darmstadt, Germany). A Spherisorb® ODS-2 column (25 cm x 4.6 mm, 5 μm particle size; Waters, Milford, MA, USA) with a LiChropher® 100-RP-18 guard cartridge was used for the separation of pigments, applying a gradient according to Wright et al. (1991). Peaks were detected at 440 nm and identified as well as quantified by co-chromatography with standards for Allo, Chl *a* and c2 (DHI Lab Products, Hørsholm, Denmark) using the software EZChrom Elite ver. 3.1.3. (Agilent Technologies, Santa Clara, CA, USA). Pigment contents were normalized to filtered volume and cell densities to yield cellular quotas.

2.5 Statistics

Combined effects of the two pCO_2 (ambient and OA) and light (LL, ML, and HL) treatments on all experimental parameters were statistically analyzed using two-way analyses of variance (ANOVA) with Bonferroni's multiple comparison post tests. To test for significant differences between light treatments of the OA-grown cells of *G. cryophila* cells one-way ANOVAs with additional Bonferroni's multiple comparison post tests were applied. All statistical analyses were performed using the program GraphPad Prism (Version 5.00 for Windows, Graph Pad Software, San Diego California, USA) and the significance testing was done at the $p < 0.05$ level.

3 Results

3.1 Seawater carbonate chemistry

The two target pCO_2 levels of 400 and 1000 µatm were successfully achieved for abiotic control (abiotic, bubbled seawater without cells) and culture bottles (biotic, 1-*way ANOVA*: $p < 0.0001$, Table 1). As the pCO_2 of the abiotic control and culture bottles of the same pCO_2 treatment were similar, this indicates that final cell numbers of *G. cryophila* did not alter the pCO_2 of the culture bottles relative to the culture medium. Similar trends as for the pCO_2 were also apparent for the measured pH values, which yielded 8.13 ± 0.07 and 7.82 ± 0.06 in the culture bottles of the ambient and OA treatments, respectively (Table 1). While DIC concentrations were significantly enhanced for OA relative to the ambient pCO_2 treatments (1-*way ANOVA*: $p < 0.0001$), they also significantly differed between abiotic control (abiotic, bubbled seawater without cells) and culture bottles (biotic, Table 1).

3.2 Growth, elemental stoichiometry and composition

Growth rates were significantly affected by light (*2-way ANOVA*: $p = 0.002$), but not by OA (Fig. 1A). In response to increasing irradiance, growth rates remained unchanged in cells grown under ambient pCO_2, but significantly increased under OA between LL and ML by 89% (posthoc: $p < 0.05$) and between ML and HL by 32% (posthoc: $p < 0.05$), respectively. Irrespective of changes in irradiance or pCO_2, cellular POC contents did not change (Fig. 1B). Daily POC production rates, were, however, significantly altered by increasing irradiance (*2-way ANOVA*: $p < 0.01$), but not by OA (Fig. 1C). While increasing light intensity did not affect POC production rates of the ambient pCO_2 treatments, there was a significant OA-dependent enhancement by 69% between LL and ML (posthoc: $p < 0.01$) and by 39% between ML and HL, respectively (posthoc: $p < 0.05$). Molar C:N ratios were significantly influenced by the interaction of both factors together (*2-way ANOVA*: $p < 0.01$; Fig. 1D). From LL to ML C:N ratios did not

change for all pCO_2 treatments whereas from ML to HL the ratio declined by 12% for the OA treatment (*1-way ANOVA*: $p < 0.05$). In response to increasing pCO_2, C:N decreased by 10% when grown under LL (posthoc: $p < 0.05$), but remained unaltered at ML.

3.3 Pigments

For all pCO_2 treatments, cellular concentrations of the measured pigments (Allo, Chl *a* and c_2) showed a strong and significant decline between LL and ML (*2-way ANOVA*: $p < 0.0001$, Table 2). Between ML and HL, however, different effects were seen, with a significant enhancement for Chl *a* (posthoc: $p < 0.01$) and Allo (posthoc: $p < 0.01$) and no effect for Chl c_2. Increasing pCO_2 had generally no effect on cellular pigment quotas (Allo, Chl *a* and c_2) except for the Allo quotas of the LL treatments, which displayed a significant OA-dependent decline by 26% (posthoc: $p < 0.01$).

3.4 Chlorophyll *a* fluorescence

The dark-adapted maximum quantum yield of PSII (F_v/F_m) was strongly influenced by irradiance (*2-way ANOVA*: $p < 0.0001$) and CO_2 (*2-way ANOVA*: $p = 0.0012$) and their interaction (*2-way ANOVA*: $p < 0.05$; Fig. 2A). For all pCO_2 treatments, increasing irradiance negatively affected F_v/F_m, with the lowest value determined for HL acclimated cells in conjunction with OA. With increasing pCO_2, F_v/F_m was increased by 17% at LL (posthoc: $p < 0.01$), but did not change at ML. Comparing the F_v/F_m measured before and after the FLC-curve, the F_v/F_m recovery was calculated and given as % of the initial F_v/F_m. F_v/F_m recovery was affected by increasing irradiance (*2-way ANOVA*: $p < 0.01$), but not pCO_2 (Fig. 2B). Except for the ambient pCO_2 treatment, which showed a significant enhancement by 11% between LL and ML (posthoc: $p < 0.05$), the increase in light did not alter F_v/F_m recovery. Changes in pCO_2 did also not alter F_v/F_m recovery.

From LL to ML, cellular concentrations of functional photosystem II reaction centers ([RCII]) decreased by 39% in the ambient pCO_2 (posthoc: $p < 0.001$) while they increased by 44% in the OA treatment (posthoc: $p < 0.01$, Fig. 3). Between ML and HL, however, [RCII] remained unaltered for the OA treatment. As a result from OA, [RCII] declined by 37% at LL (posthoc: $p < 0.01$), but was stimulated by 49% at ML (posthoc: $p < 0.01$).

While the energy transfer between PSII units (i.e. connectivity, *P*) did not change between LL and ML for the ambient pCO_2 treatment, a light-dependent decline by 22% was seen for the OA treatment (posthoc: $p < 0.05$, Table 3). Between ML and HL, *P* remained unaltered in the OA treatment. For all light treatments, no OA effect was found. From LL to ML, functional absorption cross-sections of PSII (σ_{PSII}) were similar large at ambient pCO_2, but were reduced by 8% under OA (posthoc: $p < 0.05$, Table 3). Only between ML and HL, σ_{PSII} significantly increased by 18% in the OA treatment (posthoc: $p < 0.01$). While an OA-dependent enhancement of σ_{PSII} by 10% was observed under LL (posthoc: $p < 0.05$), such change was not found under ML. Re-oxidation times of the primary electron acceptor Q_a (τ_{Qa}) were generally not affected by increasing irradiance or pCO_2 (Table 3). Only when grown under OA, the re-oxidation time was shorter by 12% between ML and HL (posthoc: $p < 0.05$).

Absolute ETRs differed in amplitude and shape in response to the applied changes in irradiance and pCO_2 (Fig. 4). Both maximum absolute electron transport rates (ETR_{max}) and minimum saturating irradiances (I_K) increased from LL to ML in the ambient pCO_2 treatment (ETR_{max}: posthoc: $p < 0.05$, I_K: posthoc: $p < 0.05$) while both parameters remained unchanged under these conditions in the OA treatment (Fig. 4, Table 3). Similarly, ETR_{max} and I_K of the OA treatment did not differ between ML and HL. Increasing pCO_2 affected ETR_{max} and I_K, but only under LL, where both parameters showed a significant enhancement (ETR_{max}: posthoc: $p < 0.05$, I_K: posthoc: p

< 0.05). From LL to ML, the maximum light utilization efficiency (α) significantly increased by 53% in the ambient pCO_2 treatment (posthoc: $p < 0.01$), but remained unchanged in the OA treatment (Table 3). Between ML and HL, α did not differ when grown under OA. A significant OA effect was only observed for the ML treatment, where α significantly declined by 23% (posthoc: $p < 0.05$, Table 3).

Nonphotochemical quenching (NPQ) generally went up with increasing actinic irradiance during the FLC (Fig. 5). Compared with the LL treatments, NPQ values of the ML and HL treatments were as twice as high (Fig. 5). There were no differences in the NPQ pattern between ML and HL treatments observed. While pCO_2 had no effect on NPQ in the ML treatments, much higher NPQ values were determined in the ambient pCO_2 relative to the OA treatment.

4 Discussion

4.1 *Geminigera cryophila* is sensitive to increasing irradiance under ambient pCO_2

The cryptophyte *G. cryophila* was well adapted to grow under LL and ML at ambient pCO_2, yielding similar growth, POC quotas and production rates as well as C:N ratios (Fig. 1). In line with this, the exposure of the cryptophyte *Rhodomonas salina* to 30 up to 150 μmol photons m^{-2} s^{-1} did not lead to any changes in growth rate at 5 °C (Hammer et al., 2002). Even though growth and biomass remained unchanged in *G. cryophila* between LL and ML, acclimation to the even higher light intensity of 500 μmol photons m^{-2} s^{-1} was indicated by the reduction in F_v/F_m and [RCII] (Figs. 2A, 3). Such decline in the number of photosystems is a typical photoacclimation response of most microalgae to increasing light and is usually accompanied by a decrease in cellular concentrations of light harvesting pigments (MacIntyre et al., 2002), as seen here for cellular Chl *a* and c_2 quotas (Table 2). Even though most studies on temperate cryptophytes report a photoprotective function of Allo, with higher amounts of this carotenoid toward high irradiance (Funk et al., 2011; Laviale and Neveux, 2011), the reduction in cellular Allo quotas from LL to ML in our tested species (Table 2) rather suggests its role in light absorption. Similarly, cellular Allo contents also declined between 40 and 100 μmol photons m^{-2} s^{-1} in the temperate cryptophyte *Rhodomonas marina* (Henriksen et al., 2002). In this study, various photophysiological parameters (P, σ_{PSII}, τ_{Qa}) did not change between LL and ML in *G. cryophila* while other photoacclimation processes such as higher ETR_{max}, I_k and α took place (Table 3). Such light-dependent apparent higher electron flow was accompanied by similar high POC quotas and production rates between LL and ML (Fig. 1B, C) and suggests saturation of the Calvin cycle and therewith the requirement for alternative electron cycling to dissipate the excessive light energy. In the temperate *R. salina*, the onset of NPQ was induced after saturation of the Calvin cycle and found to be located in the chlorophyll a/c proteins and not in the phycobiliproteins (Kana et al., 2012). In fact, NPQ was strongly enhanced in *G. cryophila* between LL and ML at ambient pCO_2 (Fig. 5). As ML- relative to LL-acclimated cells also exhibited a higher potential of F_v/F_m recovery after the FLC curve (Fig. 2B), it appears that all these adjustments allowed a reduction of the excitation pressure on the photosynthetic apparatus and protected *G. cryophila* well against short-term high light exposure. Unexpectedly, *G. cryophila* was, however, unable to grow at the highest light intensity of 500 μmol photons m^{-2} s^{-1} under ambient pCO_2, pointing towards its vulnerability to cope with HL under present day pCO_2. Long-term field observations have shown that cryptophytes mainly occur under stratified conditions along the WAP (e.g. Moline and Prézelin, 1996; Moline et al., 2004; Mendes et al., 2013). A connection of this group with high illuminated conditions was first suggested by Mendes et al. (2017), but lacks information on their photosynthetic responses. On the basis of our results, the here tested *G. cryophila* strain was able to cope well with medium, but not high

irradiances. More tests with other cryptophytes are certainly required for being able to better evaluate cryptophytes' abilities to cope with high irradiances.

4.2 OA alters the physiological response of *G. cryophila* to high irradiance

In line with previous studies on Antarctic diatoms and *P. antarctica* (Hoogstraten et al., 2012; Heiden et al., 2016; Trimborn et al., 2017b), OA in conjunction with low irradiance did not alter growth, cellular contents or production rates of POC in *G. cryophila* (Fig. 1A-C). There was, however, an OA-dependent decline in C:N under LL (Fig. 1D), resulting from a significant enhancement of PON quotas between ambient and high pCO_2 (23.1 ± 1.4 and 29.0 ± 1.6 pg N $cell^{-1}$, respectively, posthoc: $p < 0.05$). Hence, *G. cryophila* cells most probably benefitted from lower energy investments to acquire inorganic carbon under high pCO_2. Whereas the two temperate cryptophytes *Rhodomonas* sp. and *Chroomonas* sp. (Burns and Beardall, 1987; Camiro-Vargas et al., 2005), similar to other Antarctic phytoplankton taxa (Trimborn et al., 2013), were able to actively take up CO_2 and HCO_3^-, the operation of a carbon concentrating mechanism in *G. cryophila* has not been tested so far. As typically observed for temperate phytoplankton (Hopkinson et al, 2011; McCarthy et al., 2012; Yang and Gao, 2012), the higher pCO_2 was not used to fix more POC per cell by *G. cryophila* at LL (Fig. 1B, C), but instead fuelled protein build-up through conversion of carbohydrate skeletons to proteins. N assimilation is energetically costly due to the reduction steps involved (Sanz-Luque et al., 2015), therefore the finding of elevated PON buildup under OA and LL is surprising. In line with this, ETR_{max} per PSII increased by 121% from ambient to high pCO_2 (Table 3), likely used to reduce nitrite to ammonium. Calculating overall maximum ETRs per cell ($cETR_{max} = ETR_{max}$ x [RCII], given in amol $cell^{-1}$ s^{-1}), there was also an OA-dependent increase in $cETR_{max}$ by 41% (mean value of 76 and 107 amol $cell^{-1}$ s^{-1} under ambient and high pCO_2, respectively), but this increase was comparably lower relative to ETR_{max} per PSII. The reason for this comes from the strong reduction of [RCII] between ambient and high pCO_2 at LL (Fig. 3). Next to the positive OA effect on N metabolism, also the photochemical efficiency (F_v/F_m) of *G. cryophila* was significantly increased by 17% by OA under LL (Fig. 2A). Unexpectedly, this effect was not the result of reduced cellular quotas of the light harvesting pigments (Chl *a* and c_2), as they remained the same under these conditions. Instead a significant OA-dependent decrease by 26% in the carotenoid Allo was found (Table 2), which could explain the positive OA effect on F_v/F_m. This is in line with the OA-dependent reduction in NPQ observed in LL-acclimated *G. cryophila* cells (Fig. 5), pointing towards a reduced need to dissipate excess light energy following short-term high light exposure. Overall, OA in conjunction with LL was beneficial for *G. cryophila*, with positive effects in particular on N metabolism.

The beneficial OA effect on N assimilation under LL, however, vanished at ML (Fig. 1D, 23.2 ± 3.2 and 23.2 ± 2.3 pg N $cell^{-1}$, respectively, posthoc: $p < 0.05$), probably as a result from the higher N metabolism cost to maintain photosynthesis under these conditions (Li et al., 2015). Based on our results, the physiology of the cryptophyte *G. cryophila* remained more or less unchanged between ambient and high pCO_2 at ML (Figs.1, 2, 4 and 5, Tables 2 and 3). At the highest irradiance (HL), *G. cryophila* could not grow under ambient pCO_2, but surprisingly grew well under the same light intensity in conjunction with OA, displaying highest growth rates compared to all other treatments (Fig. 1A). Similarly, this species also showed highest production rates of POC and PON (Fig. 1). Compared with the tested Antarctic diatoms and *P. antarctica* so far, which exhibited either negative or neutral effects in response to OA and high irradiance on growth and/or photosynthesis (Feng et al., 2010; Heiden et al. 2016, Trimborn et al. 2017a,b; Heiden et al. 2019; Koch et al. 2019), growth and photosynthesis of the

cryptophyte benefitted synergistically from OA and HL. Looking at the significantly higher amounts of Chl *a* and Allo per cell and its larger σ_{PSII} between ML and HL under OA (Table 2 and 3), this species even reinforced its capacity to absorb light. Faster electron drainage into downstream processes was evident by the shorter Qa re-oxidation time between ML and HL under OA (Table 2), supporting that this species indeed managed well to cope with these conditions.

4.3 Implications for the ecology of *G. cryophila* in future coastal Antarctic waters

Along the coast of the Western Antarctic Peninsula, diatoms, prymnesiophytes and cryptophytes represent the main phytoplankton groups, which form prominent blooms and therefore strongly contribute to carbon biomass build-up (Garibotti et al., 2005; Trimborn et al., 2015). Occurrence of cryptophytes in this region was associated with low salinity and warm stratified surface waters (Moline and Prézelin, 1996; Moline et al., 2004; Mendes et al., 2013; Mendes et al., 2017). Only recently, it was suggested that a high tolerance of cryptophytes to withstand high irradiances could potentially explain their occurrence in well illuminated surface waters by (Mendes et al., 2017). Our results point towards a high ability of *G. cryophila* to cope with medium, but not high irradiances, whether this applies for other Antarctic cryptophyte species as well needs further testing. With respect to the projected climatic changes, little is known about the potential CO_2 sensitivity of cryptophytes. Previous studies mainly assessed the response to OA on cryptophytes at the community level and showed no discernible effects on their abundance (Domingues et al., 2014; Sommer et al., 2015; Young et al., 2015; Schulz et al., 2017; Donahue et al., 2019). This study is the first at the species level to show that the combination of OA and high irradiance promoted growth and biomass production in the Antarctic cryptophyte *G. cryophila*. In fact, while HL conditions inhibited growth of this species under ambient pCO_2, the combination of OA and HL, on the other hand, enabled it to grow and to cope even better with the applied environmental conditions, reaching highest growth and POC production rates (Fig. 1). This was also accompanied with a high photophysiological capacity of this species when exposed on the short-term to increasing irradiances. The beneficial effect of OA and HL for *G. cryophila* is opposed to previous observations, where growth and/or photosynthesis was inhibited in several diatoms, but no effect for the prymnesiophytes *P. antarctica* (Feng et al., 2010; Trimborn et al., 2017a,b; Beszteri et al., 2018; Heiden et al., 2018; Koch et al., 2018, Heiden et al., 2019). Hence, *G. cryophila* could be a potential winner of climate change, with higher abundances and increased contribution to the productivity of future stratified, acidified and well illuminated coastal Antarctic waters. This study further confirms previous results (Moline et al., 2004; Ducklow et al., 2007; Montes-Hugo et al., 2009; Mendes et al., 2017), which point towards a stronger importance of flagellates in the future. A functional shift away from efficient carbon sinkers such as diatoms to less efficient carbon vectors such as flagellates including cryptophytes and prymnesiophytes could, however, diminish the strength of the biological carbon pump of future Antarctic coastal waters.

Author contributions

ScTr designed the study. PK conducted the experiment. ScTr, SiTh and PK analysed the data. ScTr prepared the paper with contributions from SiTh, PK and KB.

Acknowledgements

Helen Soares de Souza, Jasmin P. Heiden, Tina Brenneis and Britta Meyer are thanked for the support in the laboratory. ScTr and PK were funded by the Helmholtz association (Young Investigator Group *EcoTrace*, VH-NG-901).

References

Arrigo, K. R., van Dijken, G., and Long, M.: Coastal Southern Ocean: A strong anthropogenic CO_2 sink, Geophys. Res. Lett., 35, 1-6, doi:10.1029/2008GL035624, 2008.

Beszteri, S., Thoms, S., Benes, V., Harms, L., and Trimborn, S.: Acclimation to ocean acidification and high light in three Southern Ocean phytoplankton species: A transcriptomic study, Protist, 169, 958-975, doi:10.1016/j.protis.2018.08.003, 2018.

Burns, B. D., and Beardall, J.: Utilization of inorganic carbon by marine microalgae. J. Exp. Mar. Biol. Ecol., 107, 75-86, 1987.

Camiro-Vargas, T. K., Hernandez-Ayon, J. M., Valenzuela-Espinoza, E., Delgadillo-Hinojosa, F., and Cajal-Medrano, R.: Dissolved inorganic carbon uptake by *Rhodomonas* sp. and *Isochrysis aff. galbana* determined by a potentiometric technique, Aquacultural Engineering, 33, 83-95, 2005.

Dickson, A. G., and Millero, F. J.: A comparison of the equilibrium constants for the dissociation of carbonic acid in seawater media, Deep Sea Res., 34, 1733-1743, doi:10.1016/0198-0149(87)90021-5, 1987.

Domingues, R. B., Guerra, C. C., Barbosa, A. B., Brotas, V., Galvao, H. M., and Notes, A..: Effects of ultraviolet radiation and CO_2 increase on winter phytoplankton assemblages in a temperate coastal lagoon, J. Plankton Res., 36, 672-684, doi:10.1093/plankt/fbt135, 2014.

Donahue, K., Klaas, C., Dillingham, P.W., and Hoffmann, L.J.: Combined effects of ocean acidification and increased light intensity on natural phytoplankton communities from two Southern Ocean water masses, J. Plankton Res., 41(1), 30-45, doi:10.1093/plankt/fby048, 2019.

Ducklow, H. W., Baker, K. , Martinson, D. G., Quetin, L. B., Ross, R. M., Smith, R. C., Stammerjohn, R. C., Vernet, M., and Fraser W.: Marine pelagic ecosystems: the West Antarctic Peninsula. Phil. Trans. Roy. Soc. B: Biol. Sci., 362, 67-94, 2007.

Ducklow, H.W., Fraser, W.R., Meredith, M.P., Stammerjohn, S.E., Doney, S.C., Martinson, D.G., Sailley, S.F., Schofield, O.M., Steinberg, D.K., Venables, H.J., and Amsler, C.D.: West Antarctic Peninsula: An ice-dependent coastal marine ecosystem in transition, Oceanography, 26, 190-203, doi:10.5670/oceanog.2013.62, 2013, 2013.

Feng, Y., Hare, C. E., Rose, J. M., Handy, S. M., DiTullio, G. R., Lee, P. A., Smith, W. O., Peloquin, J., Tozzi, S., Sun, J., Zhang, Y., Dunbar, R. B., Long, M. C., Sohst, B., Lohan, M., and Hutchins, D. A.: Interactive effects of iron, irradiance and CO_2 on Ross Sea phytoplankton, Deep Sea Res. Part I Oceanogr. Res. Pap., 57, 368-383, doi:10.1016/j.dsr.2009.10.013, 2010.

Funk, C., Alami, M., Tibiletti, T., and Green, B. R.: High light stress and the onehelix LHC-like proteins of the cryptophyte *Guillardia theta*. Biochim. Biophys. Acta – Bioenerg., 1807, 841-846, 2011.

Genty, B., Briantais, J.-M., and Baker, N. R.: The relationship between the quantum yield of photosynthetic electron transport and quenching of chlorophyll fluorescence, Biochim. Biophys. Acta, 990, 87-92, doi:10.1016/S0304-4165(89)80016-9, 1989.

Gould, S. B., Waller, R. F., and McFadden, G. I.: Plastid evolution. Annu. Rev. Plant Biol. 59, 491-517, 2008.

Guillard, R. R. L., and Ryther, J. H.: Studies of marine planktonic diatoms: I. *Cyclotella nana* Hustedt, and *Detonula confervacea* (Cleve) Gran. Can. J. Microbiol., 8, 229-239, doi:10.1139/m62-029, 1962.

Hammer, A., Schumann, R., and Hendrik Schubert Light and temperature acclimation of *Rhodomonas salina* (Cryptophyceae): Photosynthetic performance, Aquat. Microb. Ecol., 29, 287-296, doi:10.3354/ame029287, 2002.

Heiden, J. P., Völkner, C., Jones, E., Van de Poll, W. H., Buma A. G. J., Meredith, M. P., De Baar, H., Bischof, K., Wolf-Gladrow, D., Trimborn, S.: Impact of ocean acidification and high solar radiation on productivity and species composition of a late summer phytoplankton community of the coastal Western Antarctic Peninsula. Limnol. Oceanogr., doi:10.1002/lno.11147, 2019.

Heiden, J. P., Thoms, S., Bischof, K., Trimborn, S.: Ocean acidification stimulates particulate organic carbon accumulation in two Antarctic diatom species under moderate and high solar radiation, J. Phycol., 54, 505-517, doi:10.1111/jpy.12753, 2018.

Heiden, J. P., Bischof, K., Trimborn, S.: Light intensity modulates the response of two Antarctic diatom species to ocean acidification, Front. Mar. Sci., 3, 260, doi: 10.3389/fmars.2016.00260, 2016.

Henriksen, P. Riemann, B., Sorensen, H. M., and Sorensen, H. L.: Effects of nutrient-limitation and irradiance on marine phytoplankton pigments, J. Plankton Res., 24, 9, 835-858, 2002.

Hopkinson, B. M., Dupont, C. L., Allen, A. E., Morel, F. M. M.: Efficiency of the CO_2-concentrating mechanism of diatoms, Proc. Natl. Acad. Sci. USA, 108, 3830-3837, 2011.

Hoogstraten, A., Timmermans, K. R., and de Baar, H. J. W.: Morphological and physiological effects in *Proboscia Alata* (Bacillariophyceae) grown under different light and CO_2 conditions of the modern Southern Ocean, J. Phycol., 48, 559-568, doi:10.1111/j.1529-8817.2012.01148.x, 2012.

Kana, R., Kotabova, E., Sobotka, R., Prasil, O.: Non-photochemical quenching in cryptophyte alga *Rhodomonas salina* is located in chlorophyll a/c antennae, PLoS ONE, 7(1), e29700,doi:10.1371/journal.pone.0029700, 2012.

Kolber, Z. S., Prášil, O., and Falkowski, P. G.: Measurements of variable chlorophyll fluorescence using fast repetition rate techniques: Defining methodology and experimental protocols, Biochim. Biophys. Acta, 1367, 88-106, doi:10.1016/S0005-2728(98)00135-2, 1998.

Koch, F., Beszteri, S., Harms, L., Trimborn, S.: The impacts of iron limitation and ocean acidification on the cellular stoichiometry, photophysiology and transcriptome of *Phaeocystis antarctica*, Limnol Oceanogr,, doi:10.1002/lno.11045, 2018.

Laviale, M., and Neveux, J.: Relationships between pigment ratios and growth irradiance in 11 marine phytoplankton species, Mar. Ecol. Prog. Ser., 425, 63-77, doi: 10.3354/meps09013, 2011.

Li, G., Brown, C. M., Jeans, J. A., Donaher, N. A., McCarthy, A., and Campbell, D. A.: The nitrogen costs of photosynthesis in a diatom under current and future pCO_2. New Phytol., 205, 533-543, doi: 10.1111/nph.13037, 2015.

MacIntyre, H. L., Kana, T. M., Anning, T., and Geider, R. J.: Photoacclimation of photosynthesis irradiance response curves and photosynthetic pigments in microalgae and cyanobacteria, J. Phycol., 38, 17-38, doi:10.1046/j.1529-8817.2002.00094.x, 2002.

McCarthy, A., Rogers, S. P., Duffy, S. J., and Campbell, D. A.: Elevated carbon dioxide differentially alters the photophysiology of *Thalassiosira pseudonana* (Bacillariophyceae) and *Emiliania huxleyi* (Haptophyta), J.

Phycol., 48, 635-646, 2012.

Mehrbach, C., Culberson, C. H., Hawley, J. E., and Pytkowicz, R. M.: Measurement of the apparent dissociation constants of carbonic acid in seawater at atmospheric pressure, Limnol. Oceanogr., 18, 897-907, doi:10.4319/lo.1973.18.6.0897, 1973.

Mendes, C. R. B., Tavano, V. M., Leal, M. C., de Souza, M. S., Brotas, V., and Garcia, C. A. E.: Shifts in the dominance between diatoms and cryptophytes during three late summers in the Bransfield Strait (Antarctic Peninsula), Polar Biol., 36, 537-547, doi:10.1007/s00300-012-1282-4, 2013.

Mendes, C. R. B., Tavano, V. M., Dotto, T. S., Kerr, R., De Souza, M. S., Garcia, C. A. E. and Secchi, E. R.: New insights on the dominance of cryptophytes in Antarctic coastal waters: A case study in Gerlache Strait, Deep Sea Res. Part II: Topical Studies Oceanogr., doi:10.1016/j.dsr2.2017.02.010, 2017.

Moline, M. A., and Prézelin, B. B.: Long-term monitoring and analyses of physical factors regulating variability in coastal Antarctic phytoplankton biomass, *in situ* productivity and taxonomic composition over seasonal and interannual timescales, Mar. Ecol. Prog. Ser., 145, 143-160, doi:10.3354/Meps145143, 1996.

Moline, M. A., Claustre, H., Frazer, T. K., Schofield, O., and Vernet, M.: Alteration of the food web along the Antarctic Peninsula in response to a regional warming trend, Glob. Change Biol., 10, 1973-1980, doi: 10.1111/j.1365-2486.2004.00825, 2004.

Montes-Hugo, M., Doney, S.C., Ducklow, H.W., Fraser, W.R., Martinson, D.G., Stammerjohn, S.E., and Schofield, O.: Recent changes in phytoplankton communities associated with rapid regional climate change along the western Antarctic Peninsula, Science 323: 1470-1473, doi:10.1126/science.1164533, 2009.

Moreau, S., Mostajir, B., Bélanger, S., Schloss, I. R., Vancoppenolle, M., Demers, S., and Ferreyra, G. A.: Climate change enhances primary production in the western Antarctic Peninsula, Glob. Change Biol., 21, 2191-2205, doi: 10.1111/gcb.12878, 2015.

Orr, J. C., V. J. Fabry, O. Aumont, L. Bopp, S. C. Doney, R. A. Feely, A. Gnanadesikan, N. Gruber, Ishida, A., Joos, F., Key, R. M., Lindsay, K., Maier-Reimer, E., Matear, R., Monfray, P., Mouchet, A., Najjar, R. G., Plattner, G.-K., Rodgers, K. B., Sabine, C. L., Sarmiento, J. L., Schlitzer, R., Slater, R. D., Totterdell, I. J., Weirig, M.-F., Yamanaka, Y., and Yool, A.: Anthropogenic ocean acidification over the twenty-first century and its impact on calcifying organisms, Nature, 437, 681-686, 2005.

Oxborough, K., Moore, C. M., Suggett, D. J., Lawson, T., Chan, H. G., and Geider, R. J.: Direct estimation of functional PSII reaction center concentration and PSII electron flux on a volume basis: a new approach to the analysis of Fast Repetition Rate fluorometry (FRRf) data, Limnol. Oceanogr. Methods, 10, 142-154, doi:10.4319/lom.2012.10.142, 2012.

Pachauri, R.K., and Meyer, L.A. (Eds.): Climate Change 2014: Synthesis Report., ed. Contribution of workinggroups I, II and III to the fifth assessment report of the intergovernmental panel on climate change, Geneva, Switzerland, 2014.

Pierrot, D., Lewis, E., and Wallace, D. W. R.: MS Excel program developed for CO_2 system calculations, 2006.

Ralph, P. J., and Gademann, R.: Rapid light curves: A powerful tool to assess photosynthetic activity, Aquat. Bot., 82, 222-237, doi:10.1016/j.aquabot.2005.02.006, 2005.

Redfield, A. C.: The biological control of chemical factors in the environment, Am. Sci., 64, 205–221, doi:10.2307/27828530, 1958.

Rozema, P. D., Venables, H. J., van de Poll, W. H., Clarke, A., Meredith, M. P., and Buma, A. G. J.: Interannual variability in phytoplankton biomass and species composition in northern Marguerite Bay (West Antarctic Peninsula) is governed by both winter sea ice cover and summer stratification, Limnol. Oceanogr., 62, 235-252, 2017.

Sanz-Luque, E., Chamizo-Ampudia, A., Llamas, A., Galvan, A. and Fernandez, E.: Understanding nitrate assimilation and its regulation in microalgae, Front. Plant Sci., 6, 899, doi: 10.3389/fpls.2015.00899, 2015.

Schulz, K. G., Bach, L. T., Bellerby, R. G. J., Bermúdez, R., Büdenbender, J., Boxhammer, T., Czerny, J., Engel, A., Ludwig, A., Meyerhöfer, M., Larsen, A., Paul, A. J., Sswat, M. and Riebesell, U.: Phytoplankton blooms at increasing levels of atmospheric carbon dioxide: Experimental evidence for negative effects on prymnesiophytes and positive on small picoeukaryotes, Front. Mar. Sci., 4, 64, doi:10.3389/fmars.2017.00064, 2017.

Smith, R. C., and S. E. Stammerjohn.: Variations of surface air temperature and sea-ice extent in the western Antarctic Peninsula region, Ann. Glaciol., 33, 493-500, doi:10.3189/172756401781818662, 2001.

Sommer, U., Paul, C., Moustaka-Gouni, M. Warming and ocean acidification effects on phytoplankton - From species shifts to size shifts within species in a mesocosm experiment, PLoS ONE, 10(5), e0125239, doi:10.1371/journal.pone.0125239, 2015.

Stoll, M. H. C., Bakker, K., Nobbe, G. H., and Haese, R. R. Continous-flow analysis of dissolved inorganic carbon content in seawater, Analaytical Chem., 73, 4111-4116, doi:10.1021/ac010303r, 2001.

Suggett, D. J., MacIntyre, H. L., and Geider, R. J.: Evaluation of biophysical and optical determinations of light absorption by photosystem II in phytoplankton, Limnol. Oceanogr. Methods, 2, 316-332, doi:10.4319/lom.2004.2.316, 2004.

Suggett, D. J., Moore, C. M., Hickman, A. E., and Geider, R. J.: Interpretation of fast repetition rate (FRR) fluorescence: Signatures of phytoplankton community structure versus physiological state, Mar. Ecol. Prog. Ser., 376, 1-19, doi:10.3354/meps07830, 2009.

Trimborn, S., Brenneis, T., Sweet, E., Rost, B.: Sensitivity of Antarctic phytoplankton species to ocean acidification: growth, carbon acquisition and species interaction, Limnol. Oceanogr., 58, 997-1007, 2013.

Trimborn, S., Hoppe, C. J. M., Taylor, B., Bracher, A., Hassler, C.: Physiological characteristics of phytoplankton communities of Western Antarctic Peninsula and Drake Passage waters, Deep Sea Res. Part I, 98, 115-124, 2015.

Trimborn, S., Brenneis, T., Hoppe, C. J. M., Norman, L., Santos, J., Laglera, L., Völkner, C., Wolf-Gladrow, D., Hassler, C.: Iron sources alter the response of Southern Ocean phytoplankton to ocean acidification, Mar. Ecol. Prog. Ser., 578, 35-50, doi:10.3354/meps12250, 2017a.

Trimborn, S., Thoms, S., Brenneis, T., Heiden, J. P., Beszteri, S., Bischof, K.: Two Southern Ocean diatoms are more sensitive to ocean acidification and changes in irradiance than the prymnesiophyte *Phaeocystis antarctica*, Physiol. Plant., 160, 155-170, doi:10.1111/ppl.12539, 2017b.

Wright, S. W., Jeffrey, S. W., Mantoura, R. F. C., Llewellyn, C. A., Bjornland, T., Repeta, D., and Welschmeyer, N.: Improved HPLC method for the analysis of chlorophylls and carotenoids from marine phytoplankton, Mar. Ecol. Prog. Ser., 77, 183-196, doi:10.3354/meps077183, 1991.

Yang, G., and Gao, K.: Physiological responses of the marine diatom *Thalassiosira pseudonana* to increased pCO_2 and seawater acidity, Mar. Environ. Res., 79, 142-151, doi:10.1016/j.marenvres.2012.06.002, 2012.

Young, J. N., Kranz, S. A., Goldman, J. A. L., Tortell, P. D., and Morel, F. M. M.: Antarctic phytoplankton down-regulate their carbon-concentrating mechanisms under high CO_2 with no change in growth rates, Mar. Ecol. Progr. Ser., 532, 13-28, 2015.

Biogeosciences Discuss., https://doi.org/10.5194/bg-2019-97
Manuscript under review for journal Biogeosciences
Discussion started: 26 March 2019

Biogeosciences
Discussions
Open Access
EGU

Table 1 Partial pressures of CO_2 (pCO_2) for the ambient and ocean acidification (OA) treatments were calculated from measured pH, concentrations of dissolved inorganic carbon (DIC), silicate and phosphate, temperature, and salinity using the CO2Sys program (Pierrot et al. 2006). For all parameters, values are given for the abiotic control bottles (abiotic, bubbled seawater without cells) and the culture bottles at the end of the experiment (biotic).

Target pCO_2 (µatm)		pCO_2 (µatm)		pH (NBS)		DIC (µmol kg^{-1})	
		abiotic	biotic	abiotic	biotic	abiotic	biotic
Ambient 400	pCO_2,	372 ± 18^{a}	398 ± 66^{a}	8.14 ± 0.02^{a}	8.13 ± 0.07^{a}	2024 ± 7^{a}	2062 ± 12^{b}
OA, 1000		986 ± 42^{b}	865 ± 120^{b}	7.75 ± 0.02^{b}	7.82 ± 0.06^{b}	2160 ± 7^{c}	2195 ± 16^{d}

Biogeosciences Discuss., https://doi.org/10.5194/bg-2019-97
Manuscript under review for journal Biogeosciences
Discussion started: 26 March 2019

Table 2 Cellular concentrations of chlorophyll *a* and c_2 (Chl *a* and c_2) as well as alloxanthin (Allo) were determined for *Geminigera cryophila* acclimated to ambient or high CO_2 conditions combined with low (LL), medium (ML) or high light (HL). *G. cryophila* did not grow under ambient pCO_2 and HL as indicated by ng. Photosynthetic parameters were derived from at least three independent measurements. Different letters indicate significant differences between treatments ($p < 0.05$).

Treatment	Chl *a* (fg cell^{-1})	Chl c_2 (fg cell^{-1})	Allo (fg cell^{-1})
Ambient pCO_2 LL	2358 ± 277^{a}	172 ± 33^{a}	81 ± 3^{a}
OA LL	2300 ± 25^{a}	131 ± 1^{a}	60 ± 2^{b}
Ambient pCO_2 ML	871 ± 225^{b}	75 ± 24^{b}	30 ± 8^{c}
OA ML	662 ± 22^{b}	48 ± 15^{b}	27 ± 3^{c}
Ambient pCO_2 HL	ng	ng	ng
OA HL	772 ± 85^{c}	41 ± 1^{b}	36 ± 1^{d}

Biogeosciences Discuss., https://doi.org/10.5194/bg-2019-97
Manuscript under review for journal Biogeosciences
Discussion started: 26 March 2019

Biogeosciences
Discussions
Open Access
EGU

Table 3 Energy transfers between PSII units (i.e. connectivity, *p*), functional absorption cross section of PSII photochemistry (σ_{PSII}), cellular concentrations of functional photosystem II reaction centers ([RCII]), re-oxidation times of the primary electron acceptor Q_a (τ_{Qa}), maximum absolute electron transport rates (ETR_{max}), minimum saturating irradiances (I_K), maximum light utilization efficiencies (α) and F_v/F_m recovery were determined for *Geminigera cryophila* acclimated to ambient or high CO_2 conditions combined with low (LL), medium (ML) or high light (HL). *G. cryophila* did not grow under ambient pCO_2 and HL as indicated by ng. Photosynthetic parameters were derived from at least three independent measurements. Different letters indicate significant differences between treatments ($p < 0.05$).

Treatment	*p* (rel. unit)	σ_{PSII} (nm^2)	τ_{Qa} (µs)	ETR_{max} (e^{-1} PS^{-1} s^{-1})	I_k (µmol photo m^{-2} s^{-1})	α (rel. unit)
Ambient pCO_2 LL	0.40 ± 0.03^{a}	4.10 ± 0.11^{a}	825 ± 49^{a}	126 ± 28^{a}	72 ± 9^{a}	1.75 ± 0.17^{a}
OA LL	0.41 ± 0.02^{a}	4.49 ± 0.08^{b}	798 ± 19^{a}	279 ± 52^{b}	142 ± 34^{b}	1.98 ± 0.11^{a}
Ambient pCO_2 ML	0.36 ± 0.03^{ab}	4.25 ± 0.17^{a}	744 ± 31^{a}	265 ± 77^{b}	102 ± 38^{b}	2.67 ± 0.26^{b}
OA ML	0.32 ± 0.06^{b}	4.14 ± 0.21^{a}	772 ± 40^{a}	278 ± 70^{b}	138 ± 48^{b}	2.06 ± 0.24^{a}
Ambient pCO_2 HL	ng	ng	ng	ng	ng	ng
OA HL	0.26 ± 0.04^{b}	4.89 ± 0.17^{c}	681 ± 14^{b}	379 ± 38^{b}	156 ± 40^{b}	2.50 ± 0.37^{a}

Biogeosciences Discuss., https://doi.org/10.5194/bg-2019-97
Manuscript under review for journal Biogeosciences
Discussion started: 26 March 2019

Figure legend

Figure 1 Growth rate (A), cellular content (B) and production rate (C) of particulate organic carbon (POC) and the molar ratio of carbon to nitrogen (C:N, D) for *Geminigera cryophila* acclimated to ambient (black bars) or high CO_2 (grey bars) conditions combined with low (LL), medium (ML) or high light (HL). *G. cryophila* did not grow under ambient pCO_2 and HL as indicated by ng. Values represent the means ± SD (n = 3). Different letters indicate significant differences between treatments ($p < 0.05$).

Figure 2 The dark-adapted maximum PSII quantum yield F_v/F_m (A) and the yield recovery after short-term light stress (% of initial) (B) for *Geminigera cryophila* acclimated to ambient (black bars) or high CO_2 (grey bars) conditions combined with low (LL), medium (ML) or high light (HL). *G. cryophila* did not grow under ambient pCO_2 and HL as indicated by ng. Values represent the means ± SD (n = 3). Different letters indicate significant differences between treatments ($p < 0.05$).

Figure 3 Cellular concentrations of functional photosystem II reaction centers [RCII] were determined for *Geminigera cryophila* acclimated to ambient or high CO_2 conditions combined with low (LL), medium (ML) or high light (HL). *G. cryophila* did not grow under ambient pCO_2 and HL as indicated by ng. Different letters indicate significant differences between treatments ($p < 0.05$).

Figure 4 Absolute electron transport rates (ETR) were measured in response to increasing irradiance in *Geminigera cryophila* acclimated to ambient (black circles) or high CO_2 (white circles) conditions combined with A) low (LL), B) medium (ML) or C) high light (HL). *G. cryophila* did not grow under ambient pCO_2 and HL. ETRs were obtained in three individual measurements. Values represent the means ± SD (n = 3).

Figure 5 Nonphotochemical quenching (NPQ) was determined in response to increasing irradiance in *Geminigera cryophila* acclimated to ambient (black circles) or high CO_2 (white circles) conditions combined with A) low (LL), B) medium (ML) or C) high light (HL). *G. cryophila* did not grow under ambient pCO_2 and HL. ETRs were obtained in three individual measurements. Values represent the means ± SD (n = 3)

Biogeosciences Discuss., https://doi.org/10.5194/bg-2019-97
Manuscript under review for journal Biogeosciences
Discussion started: 26 March 2019

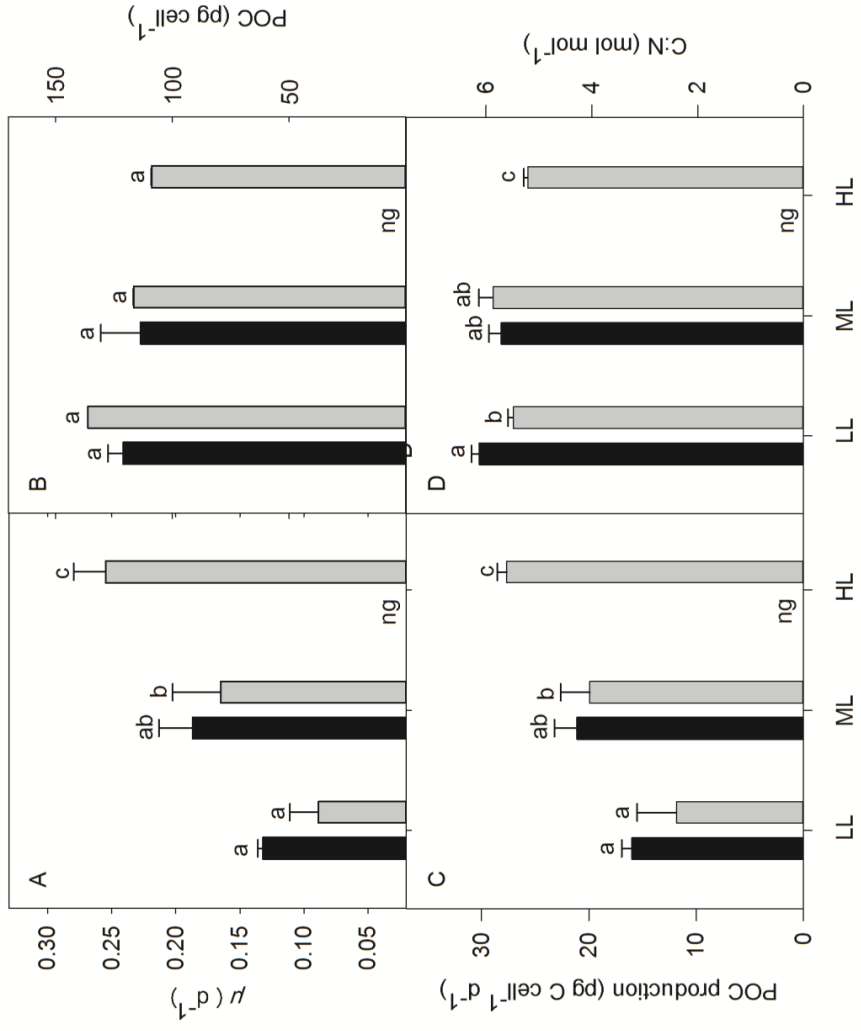

Figure 1

Biogeosciences Discuss., https://doi.org/10.5194/bg-2019-97
Manuscript under review for journal Biogeosciences
Discussion started: 26 March 2019

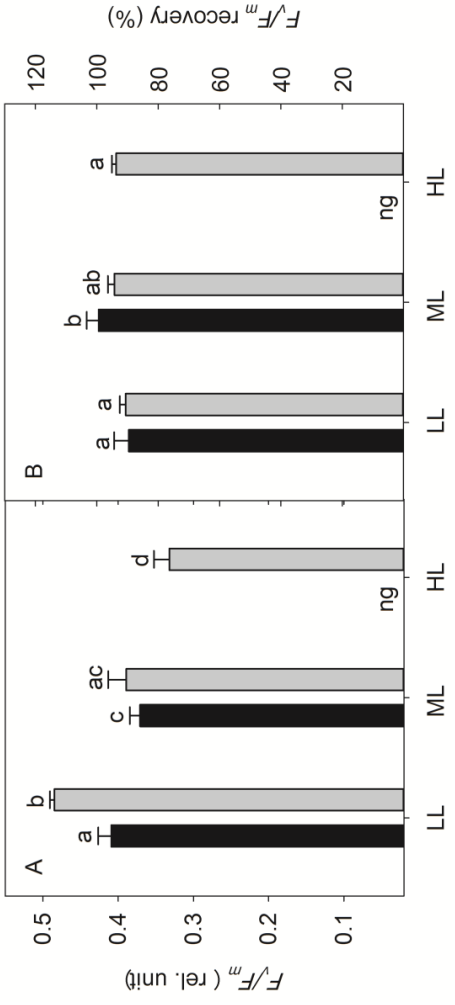

Figure 2

Biogeosciences Discuss., https://doi.org/10.5194/bg-2019-97
Manuscript under review for journal Biogeosciences
Discussion started: 26 March 2019

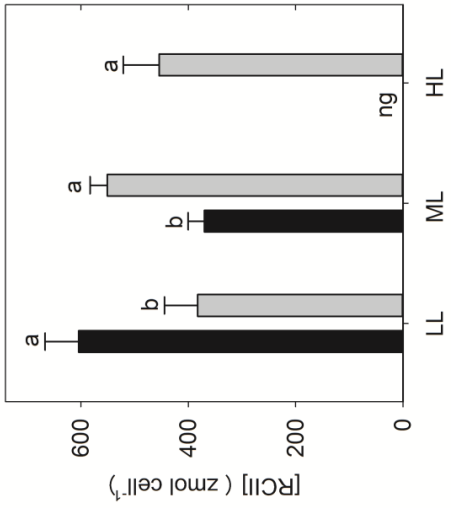

Figure 3

Biogeosciences Discuss., https://doi.org/10.5194/bg-2019-97
Manuscript under review for journal Biogeosciences
Discussion started: 26 March 2019

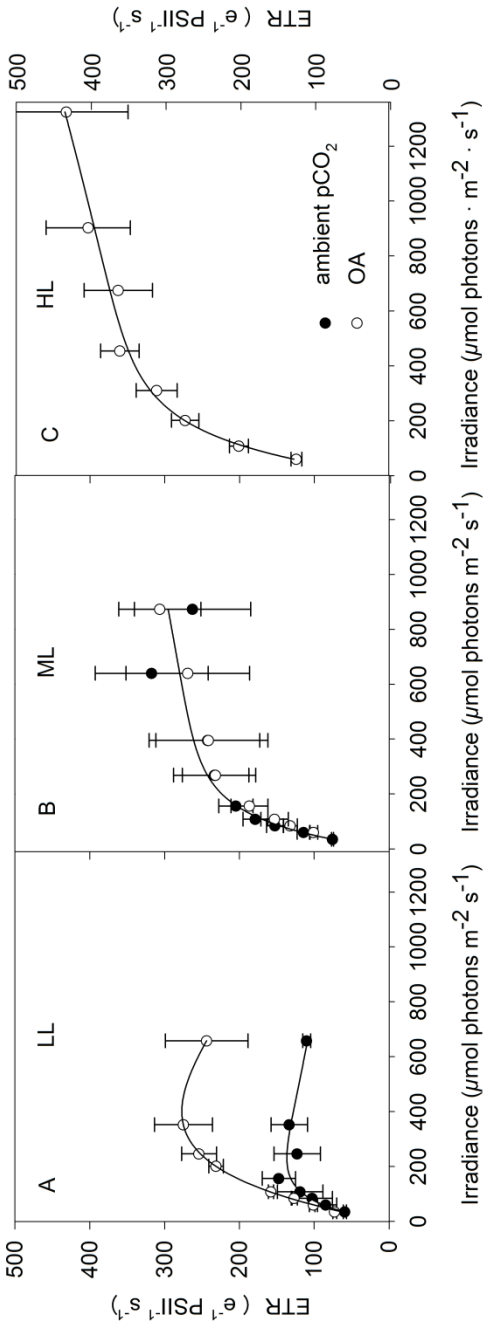

Figure 4

Biogeosciences Discuss., https://doi.org/10.5194/bg-2019-97
Manuscript under review for journal Biogeosciences
Discussion started: 26 March 2019

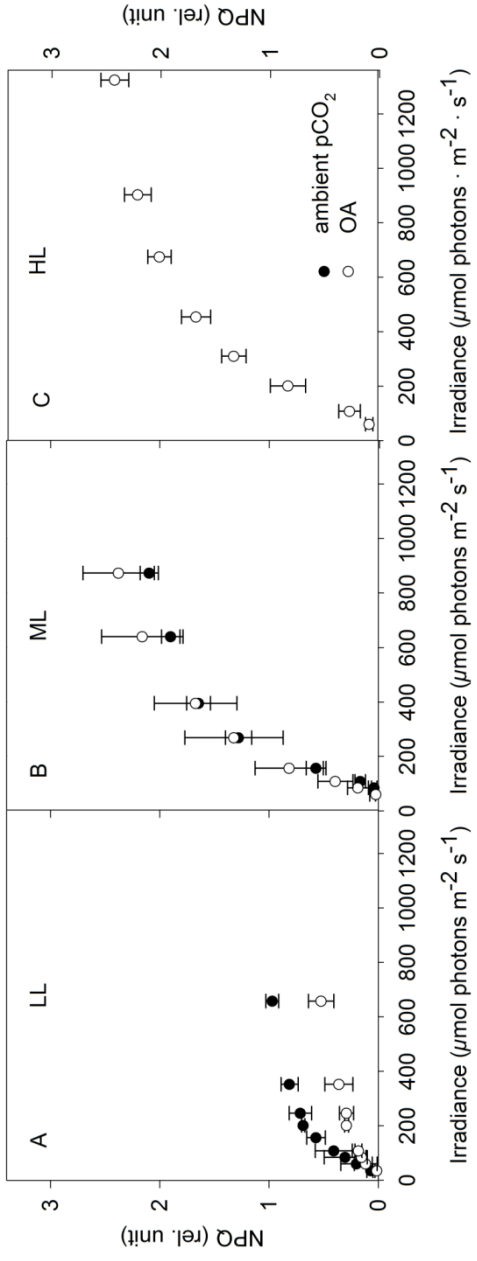

Figure 5